

# We are IntechOpen, the world's leading publisher of Open Access books Built by scientists, for scientists

4,400

Open access books available

117,000

International authors and editors

130M

Downloads

Our authors are among the

154

Countries delivered to

TOP 1%

most cited scientists

12.2%

Contributors from top 500 universities



WEB OF SCIENCE™

Selection of our books indexed in the Book Citation Index  
in Web of Science™ Core Collection (BKCI)

Interested in publishing with us?  
Contact [book.department@intechopen.com](mailto:book.department@intechopen.com)

Numbers displayed above are based on latest data collected.  
For more information visit [www.intechopen.com](http://www.intechopen.com)



## HERWIG: a Monte Carlo Program for QCD at LHC

Giuseppe Marchesini

*University of Milano–Bicocca and INFN Sezione di Milano–Bicocca, Milano  
Italy*

### 1. Introduction

Monte Carlo programs could be used for the partial description of particle physics production at high energy. These particles are hadrons, such as proton, neutron, pion and many others. They are described by QCD (quantum chromodynamics). At perturbative level QCD is formulated as gauge interaction of quarks and gluons which have color number force. They produce hadrons as physical bound states, see for instance (1). At non perturbative level, controlled numerically by computer simulations, QCD produces physical hadrons. The mass of the proton is about  $1.672 \times 10^{-27}$  kg  $\simeq 0.937$  GeV.

The FermiLab machine, see (2), has proton and antiproton running in the center of mass with an energy of 2 TeV. It was intensively operating in the last years. The FermiLab is located near Chicago.

The LHC (large hadron collider) machine is located at CERN, see (3). The machine is made of two round circles which are 27 km long. Here particles are running near Geneva between France and Switzerland. The two protons are running here one against the other with an energy of 3.5 TeV  $c^2$  so that the total mass of the colliding system is of 7 TeV. This machine started at the end of 2009. It operates until 2011 and then it will start again at a double of its present total colliding mass.

The LHC total colliding energy discloses a key point of the Standard model for particle physics, the presence of the Higgs meson which is expected with a mass between hundred and hundred and fifty time the proton mass, i.e.  $M_{\text{Higgs}}$  between 100 and 150 GeV. The Higgs meson is needed to give a simple description of the present Standard model. His absence should generate a substantial problem to this theory which unifies all elementary particle physics. A major point of the Higgs field is that it gives a mass to the weak boson Z and  $W^\pm$ . The above limit on Higgs mass are obtained from intense studies of present data on particle experiments at FermiLab, see (2), and at CERN, see (3).

The Standard model is the present theory for elementary particles, except for gravitational forces. This theory includes QCD and involves electroweak particles such as leptons (electron, muon and tau) and corresponding neutrinos. It involves photons and massive electroweak bosons as Z and  $W^\pm$ .

QCD is the theory one uses for hadron interactions. Hadrons are strong interaction particles such as baryons (as proton, nucleon etc) and mesons (as pions etc.). By perturbative description these fields interact via a gauge Lagrangian. Fields are given by partons, i.e. quark, antiquark and gluon. Hadrons are made of bound states of these elementary fields. The perturbative formulation does not allow to generate hadrons which are color singlet states of partons (color is one of parton index). QCD hadrons are generated as bound states of quarks

and gluons acting near the initial or final states. They are not reconstructed by perturbative order.

At perturbative level one needs to introduce an artificial scale  $M_0$ . Above this scale quark and gluon interaction is well definite and perturbative analysis can be done. But at low scale one has divergences for  $M_0 \rightarrow 0$  and one needs to introduce hadrons. Such an impossibility forces one to maintain a finite scale of  $M_0$ . It could be fixed by perturbative analysis and its effective value is of the order of the proton mass. Below that infrared scale  $M_0$  one has that non perturbative effects need to be involved to give hadrons in the initial or final states, but this generation of hadrons could be treated only numerically and no clear theory is still known.

One expects at the infrared scale  $M_0$  hadrons are composed as bound states of quarks and gluons. They are single states composed as color space (i.e. singlet in color space). They have a small mass and could be used to generate hadrons. Since no clear theory exists at the moment, hadrons are generated artificially. Their states are mainly close in space-time.

The perturbation theory is intensively considered in many details here. It is the basis for the Monte Carlo program called HERWIG (hadron reaction with interfering gluons). See (4). Other similar models for particle generations in these events are given in two reports in (5).

### 1.1 LHC processes and the HERWIG model

The HERWIG Monte Carlo model is essentially based on many results of perturbative QCD. It generates quarks and gluons in processes which are at short momentum distances. As we discussed above, HERWIG involves partons with an infrared artificial scale  $M_0$ . These are the relevant programs for many physical processes involving Higgs boson generation as we shall see.

An important part of the HERWIG program is the study of Higgs field which is needed to generate the mass of intermediated weak bosons  $Z$  and  $W^\pm$ . Later we will comment on this model.

The HERWIG Monte Carlo program for LHC starts from the collision of a pair of protons and generates hadrons in the final state process. It could be generalized to include general Standard model particles. Here we consider again simplifications by using only QCD processes, see later for extensions.

The Monte Carlo program is characterized by analysing processes which are at short distances or large momentum  $Q_{\text{hard}}$ . They are very important for QCD and specific for Higgs search, see later.

Each incoming proton is fragmented into three quarks at a scale  $M_0$ . One of this quarks starts the hard process by generating further partons via successive radiation which are characterized by the hard scale  $Q_{\text{hard}}$ . Later the produced final partons recombine to generate the final hadron states as recombination of final partons at soft scale  $M_0$ . HERWIG processes are then characterized by the hard physical scale  $Q_{\text{hard}}$  and the artificial scale  $M_0$ . A general picture of these collisions is then given in Fig. 1.

Here the two incoming protons are represented as black lines. Both protons have initial state emissions. Each proton emits an interacting quark of virtual mass  $M_0$  which undergoes successive emissions of quarks and gluons considered later for parton reconstruction at the end of the full cascade (see green box).

All these collisions are characterized by the hard scale  $Q_{\text{hard}}$  which enters in the hard event. The hard parameter  $Q_{\text{hard}}$  is here the momentum of emitted hard parton with respect to the incoming proton. Hard partons are generated in the hard collision at the center of this picture.

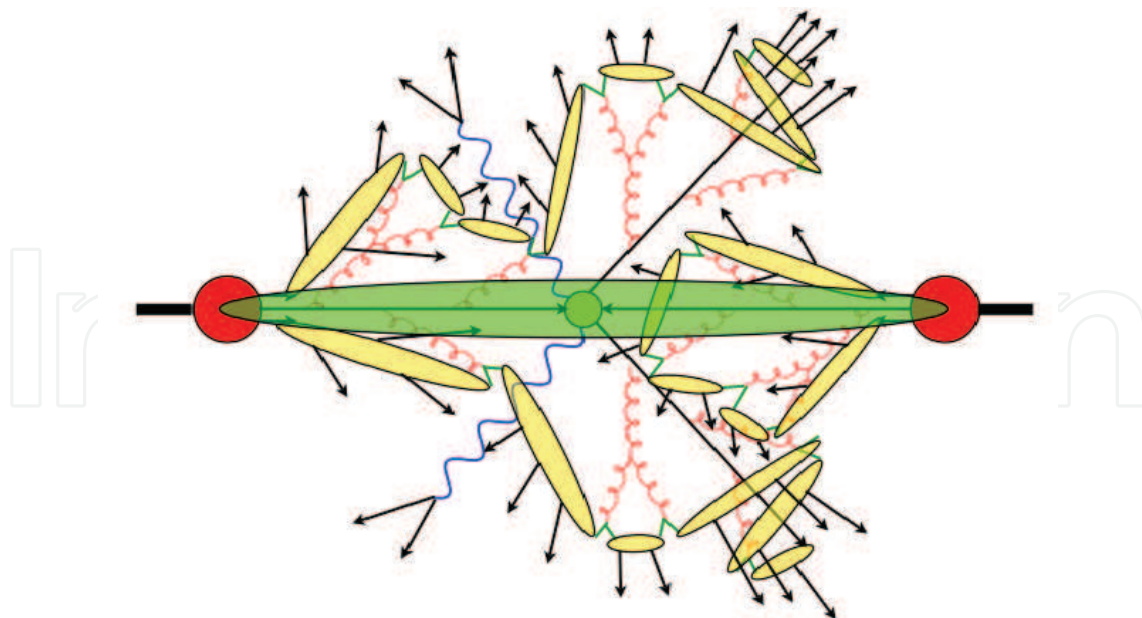


Fig. 1. LHC Monte Carlo evolution described by HERWIG program. Two protons are incoming. A proton is made of three quarks. A generation of Standard model particles is produced. Quarks are yellow and gluons are red

These partons and all other partons emitted in the initial state branching undergo successive branching into softer partons. The final emitted partons have an artificial scale  $M_0$ . They need to go under final hadron reconstructions. In the cascade a quark (a black line) undergoes gluon cascade (yellow line) which emits again gluons or quarks and antiquarks. They decay in the cascade to the soft mass  $M_0$ .

In hard collision photons are generated (green lines) and decay into a pair of electrons and positrons.

The preconfinement model force all emissions to construct hadrons in the final state (see the yellow boxes). For this reconstruction model see reference (6). Notice that incoming partons emitted by one of the incoming proton are used to reconstruct final hadrons.

One has that parton evolution and hard scattering are within perturbative QCD physics (at least to leading order). What is not included in hard QCD is the parton decay and recombination here represented as green boxes. Here hadrons are generated as from Particle Data Book, see (7).

The next picture in Fig. 2 represents the HERWIG model for the CERN machine for  $e^+e^-$  collisions. First one has the  $e^+e^-$  collision emitting a  $\gamma$  which decays into  $q\bar{q}$  starting the final state branching. Here one sees  $q \rightarrow qg$  and  $g \rightarrow gg$ . Then, after  $q\bar{q}$  formation out of each final state gluon at  $M_0$  one generates color singlet  $q\bar{q}$ . They form color singlets of small mass (see later) which cluster into hadrons which may decay. Here hadrons are generated as from Particle Data Book in (7).

### 1.2 Some indications on general evens

Complications to involve other processes in QCD or in more general theories could be here included, see (3). They could involve the full electroweak model. First of all one could generate electrons, positrons and photons and study their successive decay. Or one studies the production of weak bosons such as  $Z$  and  $W^\pm$  and their decay. In the same way one

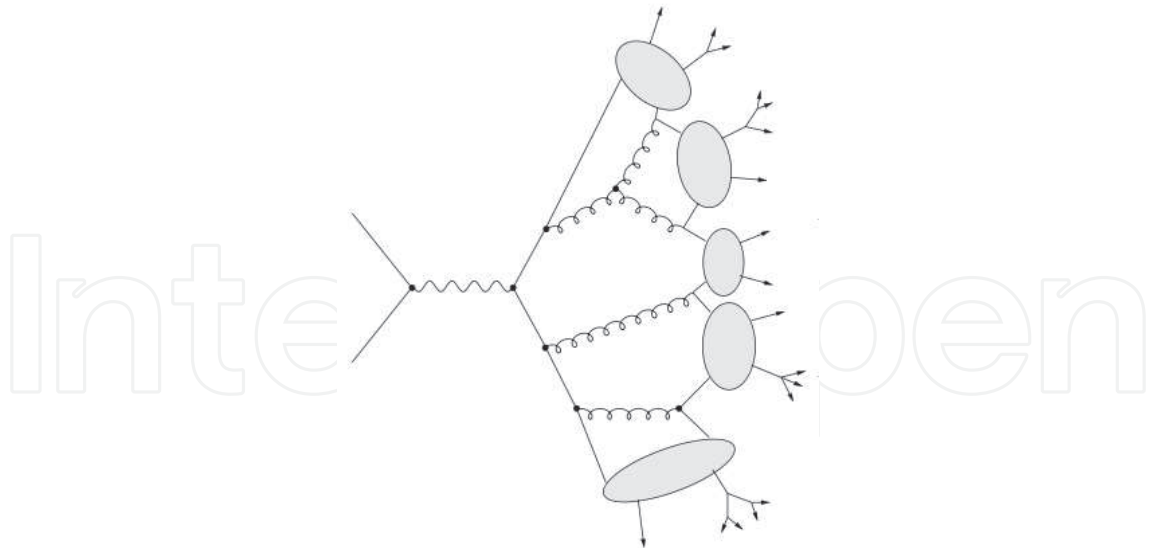


Fig. 2.  $e^+e^-$  Monte Carlo evolution in HERWIG program

involves neutrinos and antineutrinos. Finally one could include the Higgs production with its decay. This is actually the most studied program at LHC.

One could extend the model to study in HERWIG non electroweak processes as previewed by extension beyond the Standard model.

The HERWIG program has been intensively used for various processes involving other initial state particles.

#### 1.2.0.1 FermiLab machine for $p\bar{p}$ collision.

The HERWIG program was used to study proton and antiproton entering the collisions as in the collider near Chicago operating at 2 TeV. Many results have been obtained here and the HERWIG program was heavily used. See (2).

#### 1.2.0.2 DESY machine for $pe$ collision.

The HERWIG program has been used to study other type of processes. One is the electron-proton collision at DESY near Hamburg. There is an electron ring of 30 GeV running against a proton ring of 820 GeV. Here the events are studied by using essentially the HERWIG program with a different organization with one electron (or positron) as incoming particle instead of a proton in LHC. This machine proved quite well many basis of QCD, the Standard model and analyzed models beyond the Standard one. See (8).

#### 1.2.0.3 CERN machine for $e^+e^-$ collision.

The HERWIG program was also intensively used for LEP (large electron positron) at the electron-positron collision with a total energy of about 100 and 200 GeV. See (9). This  $e^+e^-$  collider was at CERN and now it is replaced by the LHC machine. Many aspects of QCD have been studied. The same for the Standard model and models beyond the Standard one. Here the electroweak particles have been intensively studied.

In all these studies HERWIG was used to consolidate the theory and in particular its strong forces. It is very interesting that many properties of perturbative QCD can be extended to all of these hard processes. Again, the missing point of the hadron formation involving the soft scale  $M_0$  are missed theoretically. They are represented as parton formation by preconfinement. For a generalization to present energies at LHC see (10).

## 2. The LHC accelerator

The LHC is a proton-proton accelerator at 7 TeV in the center of mass (it will move to 14 TeV). One of its main aim is the discovery of the neutral Higgs boson with a mass between hundred and hundred and fifty time the proton mass, i.e. between 100 and 150 GeV. In Fig. 3 one has the CERN accelerator.

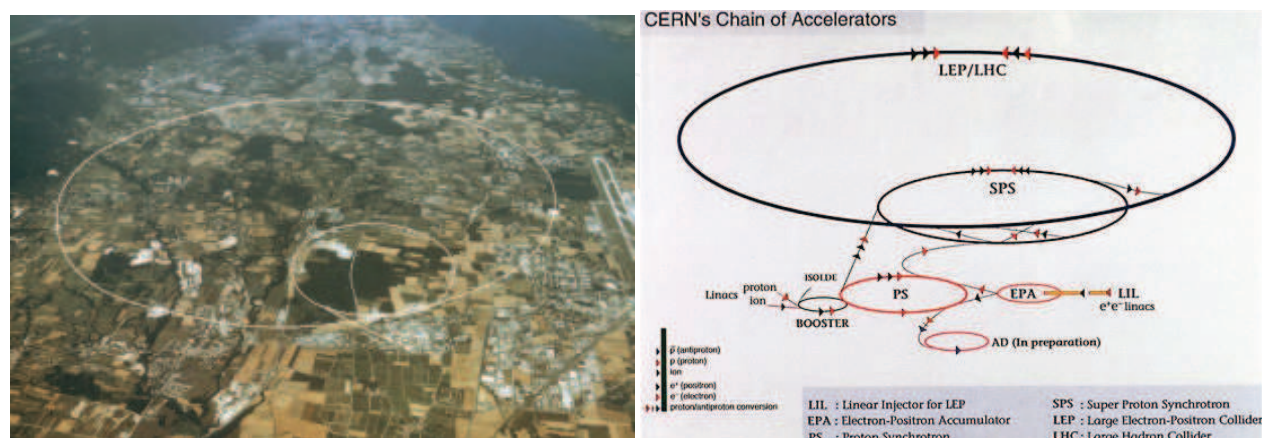


Fig. 3. The LHC accelerator at CERN

The first picture represents the structure of the accelerator which is a ring of 27 km near Geneva. The two proton beams run into two bunches one against the other. This machine started measurements at the end of 2009. The construction is schematically represented in the second picture with various other accelerators, see (3). The two proton bunches are running in opposite directions and colliding in four places. The ATLAS and CMS detectors are the two important data measurements on Standard model and beyond physics. Both collaborations have more than 3000 peoples of many countries of all continents. The other two detectors are LHCb, specialized in particular on  $b$ -meson physics measurement and ALICE, specialized on soft physics studies. See (3).

All recent CERN detectors are constructed underground, depending. The LHC/LEP machines are placed at least at 50 m underground. Similarly for the measuring four detectors.

In Fig. 3 one sees the old CERN accelerator LEP (large electron positron) which was running up to 200 GeV. Now it has been replaced by the LHC accelerator. Magnets have been changed along these years.

One sees also the SPS machine for  $p$  and  $\bar{p}$  hard collider which is now used mostly for neutrino creation and collisions at Gran Sasso detector, see (12). In the past it was used as proton antiproton accelerator as  $S\bar{p}\bar{p}s$  at 650 GeV and used for  $Z$  and  $W^\pm$  discoveries, see (3). We do not comment on the other small machines presented in the second part of in Fig. 3.

### 2.0.0.4 The LHC measurements.

At the LHC collider in Fig. 3 the ATLAS and CMS detectors are studying the Standard model physics and its possible developments. First one has the search of the Higgs boson at a supposed mass between hundred and hundred and fifty times the proton mass. The role of this "particle is to break" the gauge structure of the theory and give the measured mass to  $Z$  ( $M_Z = 91.2$  GeV) and  $W^\pm$  ( $M_W = 80.3$  GeV). All these studies are essentially done at large scale  $Q_{\text{hard}}$ . The machines used are the LEP  $e\bar{e}$  collider at 100 GeV at CERN and the FermiLab  $p\bar{p}$  collider at 2 TeV.

If this neutral Higgs meson is not found one should consider complications of the Standard model. These complications are at the moment introduced to make the Standard model more acceptable on basis of principle. Indeed the model has no theoretical control on the masses of all particles as the hadrons and electroweak particles. An important example is the very low mass of neutrinos. This can be explained within the Standard model with complications.

The HERWIG program allows the study of many processes within the Standard model and beyond. Masses have to be introduced according to PDB in (7). In particular one searches new particles at large scale not yet found. High order in QCD are also considered. New collisions are also involved here.

As mentioned one problem of the HERWIG program is the presence of the soft scale  $M_0$  previously discussed for the formation of hadrons. This is one of the key point of the HERWIG program which involves the possibility of predictions of particle emission.

A final problem in the HERWIG model at LHC is the presence of soft collision contribution at high  $Q_{\text{hard}}$ . They will not be discussed in detail in the following, but they are very important, see (3).

### 3. The HERWIG Monte Carlo program: original structure

The HERWIG Monte Carlo is based on a first perturbative order of QCD analysis of re-summed contributions to all orders of the emission of partons (quark, antiquark and gluon). It involves a large ultraviolet scale  $Q_{\text{hard}}$  and can be applied to all processes. They are:

- $e p$  collider at DESY with respective energy 30 and 820 GeV, see (8);
- $e^+e^-$  collisions at CERN with energy around 100 and 200 GeV, see (9);
- $p \bar{p}$  collider at FermiLab with total energy of 2 TeV, see (2);
- $p p$  collider at LHC with 7 TeV, see (3).

The QCD program to first order involves elementary vertexes as

$$q \rightarrow qg, \bar{q} \rightarrow \bar{q}g, g \rightarrow gg, g \rightarrow q\bar{q}. \quad (1)$$

In general two loop orders are also partially considered in HERWIG. Examples are two loops in parton splitting, next order in running coupling, higher order in parton hard collisions, etc. Important extensions are the studies of QCD infrared correction to emissions. As we shall see later they involve for instance the discussion on the scale of the running coupling.

In this paper we concentrate on a simplified form of hard QCD radiation, see (1). Complications are of course typically used in (10).

Here we mainly consider LHC collisions with proton-proton interaction. This is the running machine at CERN which will explore for instance the presence of Higgs meson. As mentioned, in LHC the total incoming momentum of the two colliding protons is now given by 7 TeV. In the future it will be 14 TeV.

One studies typically the process needed for the identification of the Higgs meson. Here one selects a large value of the ultraviolet scale  $Q_{\text{hard}}$ , typically a transverse momentum of an emitted system of particles. Many other hard scales could be involved to study specific objects or specific processes or particle production. As mentioned, both the Standard model is involved and also its extensions.

Dealing with perturbative QCD we need to introduce a soft scale  $M_0$  which is an artificial cutoff that characterizes the formation of incoming or emitting hadrons made of hard quark and gluon. This fundamental parameter characterizes our missing pieces

for the understanding of QCD. This parameter has to be fixed by perturbative analysis. Phenomenologically it turns out to be larger than the proton mass.

The picture of HERWIG program for LHC is schematically described as follows. All these pieces are at QCD perturbative order to some degree and partially extended to other models (see later).

### 3.0.0.5 Initial state cascade of proton.

We consider first the incoming quark  $k_0$  emitted by the incoming proton. Later this quark branches into additional partons  $k_1 k_2 \dots k_n$  which are either quarks, antiquarks or gluons. This branching is described by equations (1). The first incoming quark  $k_0$  has a negative mass  $Q_0^2$ . In the fragmentation an off shell quark or gluon  $k_1$  is emitted at a positive square mass  $-Q_1^2$ . One finishes with  $|Q_0^2| \ll |Q_1^2|$ . The incoming parton  $k_1$  undergoes a successive initial state branching into partons  $k_2, \dots, k_n$ . Here one has an ordered succession of decay processes with  $|Q_0^2| \ll |Q_1^2| \ll \dots \ll |Q_n^2|$ . These decays are repeated to all possible orders. Ordering is defined by Sudakov distributions of quark or gluon fragmenting (see later). The lower value is fixed at the soft scale  $M_0^2 = |Q_0^2|$ . The higher value is characterized by the hard scale  $|Q_n^2| < Q_{\text{hard}}^2$ .

### 3.0.0.6 Hard collision.

One finds the final emitted partons  $p_1$  and  $p_2$  of both incoming protons. They have large square momenta  $|Q_n^2|$  and  $|Q_m^2|$ . Note that the indices  $n$  and  $m$  are the final emitted partons in the two proton decays. They undergo a hard collision giving two partons  $p_3$  and  $p_4$

$$p_1 + p_2 \rightarrow p_3 + p_4. \quad (2)$$

This process is computed in perturbative order and then needs a perturbative calculation (first at leading order). Outgoing momenta  $p_3$  and  $p_4$  are at large positive square momenta  $Q_3^2$  and  $Q_4^2$  which are again characterized by  $Q_{\text{hard}}^2$ , depending on the selected HERWIG process. This can be generalized to include high order emission processes.

### 3.0.0.7 Final state parton branching.

At the end of the previous cascades, as described by (1), one ends up with many outgoing momenta generated in the initial stage of the fragmentation of both incoming quarks and in the outgoing momenta  $p_3$  and  $p_4$ . All these momenta are off shell as required by the cascade process. All of them will fragment by processes as  $a \rightarrow bc$  with  $a$  the successive incoming parton and  $b$  and  $c$  the outgoing partons. During this decay all partons decrease their off shell mass and via Sudakov form factors they reach the off shell artificial scale  $M_0$ .

### 3.0.0.8 Final state emission at $M_0^2$ .

Note that the soft scale  $M_0^2$  that characterizes the final emitted parton is positive. Instead the soft scale  $Q_0^2$  involved at the beginning of initial state emission of incoming protons is negative. However we set the same soft scale  $M_0^2 = -Q_0^2$  even for initial emission. In the HERWIG program the soft initial scale and the final scale are taken to be similar, but for simplicity we unify them to be the same  $M_0$ .

### 3.0.0.9 Hadron formation via preconfinement.

At the end of all these cascades one finishes with partons which are at the scale  $M_0$ . All of them form color singlets via preconfinement (see later in Fig. 7). They are parton systems which could be converted into the measured particles (mesons or baryons). This conversion



is outside a perturbative analysis and is based on intuition of the non perturbative expression of QCD.

### 3.0.0.10 Other processes.

Considerations on other processes in QCD, Standard model or non-Standard models will be discussed later.

### 3.1 The decaying incoming quark

One starts with the fragmentation of each incoming proton into three quarks. One of these is the incoming quark  $q_0$  with an artificial space-like scale with  $M_0^2 = -Q_0^2$  positive. The other two quarks are spectators and they will be considered at the end of the general branching.

The quark  $q_0$  undergoes a branching given by  $q \rightarrow qg$ . The successive branching of  $q_0$  is given by (1) and is also scaled with successive negative mass.

Consider the first process in which  $q$  at the original square scale  $|Q_0^2|$  decays into  $q'$  and  $g$ . As before they are selected according to Sudakov decomposition (see also later). There are two cases according to the fact that the quark  $q'$  or the gluon  $g$  is the second outgoing parton after the  $q$  branching.

In the first case the decaying process is  $q \rightarrow q'g$  with  $q'$  the incoming emitted quark with negative square mass  $|Q_1^2| \gg |Q_0^2|$ . Here  $g$  is the off shell emitted momentum to be discussed later for the final state emission. The distribution to one loop is given by

$$\hat{P}_{q \rightarrow qg}(z) = C_F \frac{1+z^2}{1-z}. \quad (3)$$

Here  $z$  is the fraction of the outgoing quark  $q'$  with respect to the incoming quark  $q$ .

In the second case the decaying process is the symmetric one  $q \rightarrow gq'$  with  $g$  acquiring a negative square mass  $|Q_2^2|$  which is larger than  $|Q_0^2|$ . Here the emitted quark  $q'$  is an outgoing emitted quark and will be considered later. In this case one has equation (3) but  $1-z$  is the fraction of the incoming gluon  $g$  with respect to the incoming quark  $q$ .

The chosen processes which involves  $q'$  or  $g$  are selected again by the Sudakov form factor. This expression is determined by the exponentiation of the fragmentation distribution in (2) so that the problem is here normalized in a self consistent way.

In the evolution it enter  $\alpha_s$ , the QCD running coupling. Its argument will be discussed later.

### 3.2 Fragmentation function for incoming parton

Consider an intermediated process in which the parton  $a_\ell$  with negative square momentum  $-Q_\ell^2$  is fragmenting into two partons  $a_{\ell+1}$  and  $b_{\ell+1}$ . Here  $q_{\ell+1}$  is a harder emitted initial parton. This is given by

$$a_\ell \rightarrow a_{\ell+1} b_{\ell+1}, \quad (4)$$

with  $a_\ell$  and  $a_{\ell+1}$  the ordered incoming momenta with negative squared masses  $|Q_\ell^2| \ll |Q_{\ell+1}^2|$ . Here  $b_{\ell+1}$  is the emitted parton with positive square momentum entering the final states to be considered later.

In conclusion the incoming initial quark  $q_0$  branches accord (1). Its initial state successively emitted partons  $q_1, \dots, q_n$  are bounded by the rule  $|Q_0^2| \ll |Q_1^2| \ll \dots \ll |Q_n^2|$ . Finally they will stop at a maximum value  $|Q_n^2| \ll Q_{\text{hard}}^2$ , the ultraviolet scale setting the transverse momentum of final event. The QCD vertices considered at low perturbative orders are parton decay into two partons, see (1). The Sudakov form factor is again here involved, see later.

The general splitting functions for  $a \rightarrow bc$  are given by

$$\begin{aligned}\hat{P}_{q \rightarrow qg}(z) &= C_F \frac{1+z^2}{1-z}, \\ \hat{P}_{g \rightarrow q\bar{q}}(z) &= \frac{n_f}{2} (z^2 + (1-z)^2), \\ \hat{P}_{g \rightarrow gg}(z) &= 2C_A \left( \frac{1-z}{z} + \frac{z}{1-z} + z(1-z) \right),\end{aligned}\quad (5)$$

with  $z$  the energy fraction of  $a_{\ell+1}$  with respect to the incoming hadron momentum. The coefficients  $C_F = \frac{N_c^2-1}{2N_c} = \frac{4}{3}$  and  $C_A = N_c = 3$  are given by the Casimir operators of the theory. Here  $n_f$  is the number of quark lines involved, typically less than  $n_f \leq 6$  for the  $SU(3)$  theory. Of course all these rules are valid when the quark  $q$  is replaced by the antiquark  $\bar{q}$ . The Sudakov form factors define all these selections of momenta. They are needed to satisfy sum rules. They are defined by

$$\ln S_a(Q, M_0) = - \sum_b \int_{M_0^2}^{Q^2} \frac{dq^2}{q^2} \int_{\frac{M_0}{Q}}^{1-\frac{M_0}{Q}} dz \frac{\alpha_s}{2\pi} \hat{P}_{a \rightarrow bc}(z). \quad (6)$$

The sum extends to all QCD channels. One has introduced a square momentum  $q^2$  integrated between the hard momentum  $Q^2$  (see later) and the soft one  $M_0^2$ . Also the  $z$  integration requires similar scale. In general they are integrated between  $z > \frac{M_0}{Q}$  and  $z < 1 - \frac{M_0}{Q}$  to cut off the possible singularities in the  $P$ -functions. As we will see these rules fix the appropriated sum rules for the distributions. For the soft scale  $M_0$  entering in the Sudakov factor and in the evolution, see later.

All described events are determined by leading order evolution in hard QCD. Of course higher orders need to be explored.

All descriptions are represented above by starting from the incoming momentum of the quark entering the incoming proton. In reality (see (3)) the mathematical process is fixed in an opposite way. One considers the hard scale  $Q_{\text{hard}}^2$  of the searched process. Then one fixes via Sudakov form factor the negative square scale of the last of incoming parton with momentum  $q_n$ . When  $|Q_n^2|$  is found by using (5) one starts again to determine the previous incoming momentum  $|Q_{n-1}^2|$  with similar procedure. Then one ends up to the original incoming momentum  $|Q_0^2|$ . The original branching is then fully determined by using appropriated Sudakov form factor and the selected distributions in (5).

### 3.3 General initial state evolution

Consider the fragmentation of an incoming parton  $a$  into an outgoing harder parton  $b$ . This process goes to a successive emission of intermediate incoming partons. All masses are arranged as increasing from  $a$  to  $b$ . This inclusive distribution is described as  $D_{ba}(x, Q^2)$ . Here  $Q^2$  is the hard (positive) squared momentum much larger than the soft scale  $M_0^2$ . Here  $x$  is the fraction of momentum of outgoing momentum  $b$  with respect to the incoming original parton  $a$ . The general fragmentation process assumes the general evolution equation found in (11) given by

$$Q^2 \frac{\partial}{\partial Q^2} D_{ba}(x, Q^2) = \sum_{cd} \int_x^{1-\frac{M_0}{Q}} \frac{dz}{z} \frac{\alpha_s}{\pi} P_{b \rightarrow cd}(z) D_{ca}\left(\frac{x}{z}, Q^2\right), \quad (7)$$

where the distributions  $P_{a \rightarrow bc}(z)$  are the ones described above to one loop with virtual corrections coming from  $S_a(Q, M_0)$ . They are given by

$$\begin{aligned} P_{q \rightarrow qg}(z) &= \hat{P}_{q \rightarrow qg}(z) - \delta(1-z) \int_0^{1-\frac{M_0}{Q}} dy C_F \frac{1+y^2}{1-y}, \\ P_{q \rightarrow gq}(z) &= \hat{P}_{q \rightarrow gq}(1-z), \\ P_{g \rightarrow q\bar{q}}(z) &= \hat{P}_{g \rightarrow q\bar{q}}(z), \\ P_{g \rightarrow gg}(z) &= \hat{P}_{g \rightarrow gg}(z) - \delta(1-z) \left( \int_0^{1-\frac{M_0}{Q}} dy 2C_A \frac{y}{1-y} + \frac{C_A + 2n_f}{6} \right), \end{aligned} \quad (8)$$

where a cut off  $M_0/Q$  has to be set at the maximum of  $z$  in (5) and  $y$  in (8). Note that the distributions  $P_{a \rightarrow bc}(z)$  have a  $M_0/Q$  dependence. A similar dependence appears in the distribution  $D_{ab}(z, Q)$ . This is removed when  $M_0 \rightarrow 0$  limit is taken. Here the limits at  $z = 1$  corresponds to the presence of the Sudakov form factors in the evolution equation (7). Equation (7) could be improved with two loop corrections. The running coupling  $\alpha_s$  dependence on the scale will be described below.

The Sudakov factors are defined by requiring the following sum rules. The first is the conservation of parton number when all events are generated. The second refers to the conservation of the total momentum in the same conditions. The contributions depend on the soft scale  $M_0^2$  but the sums are independent of  $M_0^2$  for small values. Of course the various sums do not depend on the hard scale  $Q^2$ .

There are various distributions for various channels. They are the following

$$D_{qq}, D_{\bar{q}q}, D_{q\bar{q}}, D_{pg}, D_{gp}, D_{gg}. \quad (9)$$

Again here one has the  $q \rightarrow \bar{q}$  symmetry. All these channels are active in the normal parton evolutions. They contribute to the various channels and could be directly measured. There are various measurements and comparisons with (7). At high energy the agreement with data is quite good. Also the sum rules are quite reliably satisfied.

Later we will discuss also the distribution for the final state evolutions. They are not different from the ones in (7) at one loop but they change both for higher loops and for the running coupling dependence on the hard scale

### 3.4 The hard collisions

At this point two partons of momenta  $p_1$  and  $p_2$  are entering our collision in (2) with negative square masses. They could be either quarks or gluons. Here  $p_1$  and  $p_2$  are the result of the successive emissions out of the two incoming protons in LHC. Here they collide according to the maximal hard scale  $Q_{\text{hard}}$  selected for this process.

As given in (2) they generate the hard collisions giving outgoing partons  $p_3$  and  $p_4$ . They could be either quarks or gluons. At this level the theory predicts, at the large scale here considered, only vertices with emissions as in (1). Other events could be used with more than two emitted partons. In all these events the partons  $p_3$  and  $p_4$  have hard momenta given by  $Q_{\text{hard}}^2$ .

The distribution (2) in QCD is taken to the perturbative order at least to zero order. Indeed the distribution is controlled by the hard scale for the process and then only low orders are relevant. Complications to higher order are also considered. One could also consider non QCD production as in the Standard model or beyond.

### 3.5 The recombination

Consider the two proton collisions in the LHC process. At this point they undergo a hard collision  $p_1 p_2 \rightarrow p_3 p_4$  as in (5). In the Monte Carlo evolution one ends with:

- partons emitted by initial state radiation leading to  $p_1$  and  $p_2$ . They are off shell and have mass much smaller than  $Q_{\text{hard}}$ ;
- partons  $p_3$  and  $p_4$  emitted in the hard collision. They have momentum much smaller than  $Q_{\text{hard}}$ .

In addition to all these off shell partons  $p_3$  and  $p_4$  and the radiation of  $p_1$  and  $p_2$  one has to consider their final state emission. According to QCD rules all these partons decay as in the usual rule with successive decaying processes  $a \rightarrow b c$  with  $a, b$  and  $c$  given by quarks, antiquarks or gluons. Here they have positive mass. They radiate by emitting additional partons according to QCD rules in (4). They radiated masses here are both positive and decrease down to  $M_0$ . This is done according to QCD rules as in (7).

As before they are selected by the Sudakov decomposition. The results are again obtained by the usual rules  $\hat{P}_{a \rightarrow bc}(z)$ . At one loop they are given in (5). Here  $z$  is the fraction of the intermediate parton momentum with respect to the incoming parton emitted by initial legs. Notice that the two outgoing momenta  $z$  and  $1 - z$  are here involved, see (5).

The Sudakov form factors are given by the exponential integrations of  $\hat{P}_{a \rightarrow bc}(z)$ . They are given in (6). It is interesting that all these expressions as the parton distributions  $P_{a \rightarrow bc}(z)$  and the Sudakov factors are the same as the incoming distributions, see by (5) and (6). However the emission distributions  $P_{a \rightarrow bc}(z)$  and Sudakov form factors  $S_a(Q, Q_0)$  differ at next to leading order in initial states and in final emissions. They have different expressions depending on the facts that they change for the  $z$  dependence and the running coupling expressions (as it would be mentioned later).

Finally one ends with many partons emitted in the final state with low momentum  $M_0$  described above. They are partons which are generated by the radiation of  $p_3$  and  $p_4$  partons in the hard collision (2). To them one adds the partons generated by decay of the hard partons  $k_1 \cdots k_n$  radiated by the intermediate emissions out of initial states. As a result all final state emissions are depending on the hard physical scale  $Q_{\text{hard}}$  and the infrared artificial  $M_0^2$ . To these final partons emitted at scale  $M_0^2$  one needs to add the pair of quark generated in the initial proton fragmentation.

Summarizing all the evolutions, one finds a succession of final states parton emitted at scale  $M_0^2$ . They come from

- splitting of finally emitted partons  $p_3$  and  $p_4$  in (2);
- splitting of  $k_1 \cdots k_n$  which are partons emitted by incoming legs;
- final state evolutions of spectator partons emitted from the two protons.

All of these final state partons are obtained by the  $a \rightarrow bc$  distributions in (5) and the Sudakov form factors in (6).

### 3.6 Color recombination into hadrons

In QCD all emitted quarks and antiquarks have a color index  $N_c = 3$ . For formal large color index  $N_c$  one has that all systems of emitted  $q$  and  $\bar{q}$  from color singlet could be converted into hadrons which do not have color index.

Consider an example of final state emission with quark and antiquark with mass close to  $M_0$ . Take such a final state emission:

- consider a quark  $q_{n-1}$  decaying into a quark  $q_n$  and a gluon  $g$ . Suppose that outgoing quark  $q_n$  has a final state mass  $M_0$ ;
- then consider the gluon  $g$  decaying into an antiquark  $\bar{q}_n$  and a quark. Suppose that outgoing antiquark  $\bar{q}_n$  has a final state mass  $M_0$ ;
- for large color  $N_c$  one has that the quark and antiquark  $q_n$  and  $\bar{q}_n$  form a large color singlet. Its mass results of the same order as  $M_0$ . This will be soon proved;
- the emitted final quark and antiquark  $q_n$  and  $\bar{q}_n$  have a color singlet for large  $N_c$ . One has that these quark and antiquark form a color singlet and could be ready to generate a hadron system (meson as quark and antiquark). Similarly for the formation of baryon (out of three quarks) or antibaryon (out of three antiquarks).

So this is the basis for HERWIG formation of hadron final states. Without entering into this perturbative analysis of QCD one could give the necessary information for preconfinement, see (6).

Consider two final state partons  $q_a$  and  $p_b$  emitted in QCD with low off-shell mass  $M_0$ . Let us assume that we do not fix the color index of  $p_a$  and  $p_b$  we sum over all of them. Their square mass  $m_{ab}^2 = (p_a + p_b)^2$  is arbitrary and simply smaller than the kinematical boundary. There are no conditions from Sudakov factor since they cancel in the real emission distribution  $P(x)$  and the Sudakov factor  $S(Q, Q_0)$ .

The situation changes when one considers two partons  $q_n$  and  $\bar{q}_n$  which are near in color as the ones described above. Here one could follow the color line of quark  $q_n$  and one ends into the anti-color of antiquark  $\bar{q}_n$  (for large color). The presence of this color separation generates a Sudakov form factor of (6) with  $M_0$  dependence.

As usual this is not cancelled by a compensation coming from the evolution vertices  $P(z)$ . This is enough to force parton  $q_n$  and  $\bar{q}_n$  to be close in momentum. This fact, resulting from the Sudakov factors in QCD, are enough to force the two partons to be close in momentum with a mass of order of  $M_0$ .

### 3.7 The physics generation

At the end of the evolution one finishes with systems of partons. They are organized in color systems of small mass of order of  $M_0$  and ready to form hadrons. Here one assumes that only quarks and antiquarks are generated in the final state. The HERWIG program is then organized in such a way to reconstruct hadrons out of these systems by using Particle Data Book in (7).

There are complications when the Sudakov distribution generates color singlet partons with mass not small enough. Here one needs to assume cluster formation according to simple rules given in (7). Of course this hadron generation is not constructed on the basis of QCD but based on reasonable principles grounded on physical considerations.

Of course other types of hadron generations are considered. They are generated in cluster of small mass color singlets of partons, see also (5).

### 3.8 Other processes

>From previous description it is clear that the HERWIG program could be extended to include other particle data, at least on perturbative level. They are for instance the followings:

- Higgs production are considered with large mass. This is one of the most important part of the Standard model which needs to be tested. They are based on the Standard model or its extensions;

- add electrodynamics predictions involving photon emission or recoils. This involves recoil of hadron or photon emission out of partons;
- the Standard model prediction with emission of weak bosons, that is  $q \rightarrow Zq$  or  $q \rightarrow W^\pm q$ ;
- similarly one could consider in HERWIG the decay of  $Z$  and  $W^\pm$  into partons, photons, fermions, neutrinos, etc.

Many more extensions could be considered by taking into account also non Standard model physics.

#### 4. The HERWIG Monte Carlo program: relevant details

Here we consider some important details in QCD theory. Most of these considerations are based on perturbative analysis. The derivations of these studies are actually based on analytical studies and included in HERWIG program. An important point in this HERWIG analysis is the presence of the infrared cutoff  $M_0$  which enters all analysis. One recalls that this is due to our ignorance of non perturbative QCD converting all parton studies into hadrons. The other important point is that processes in HERWIG program are considered by including the physical scale  $Q_{\text{hard}}$  which enters in all hard processes.

##### 4.0.0.11 The running coupling.

An important object to consider in QCD is the fact that the coupling is running in the ultraviolet region, i.e. for large momentum  $Q$ . This is universal up to two loops and given by

$$Q \frac{\partial}{\partial Q} \alpha_s(Q) = -\frac{\beta_0}{2\pi} \alpha_s^2(Q) - \frac{\beta_1}{4\pi^2} \alpha_s^3(Q) + \dots \quad (10)$$

with  $\beta_0 = 11 - \frac{2}{3} n_f$  and  $\beta_1 = 51 - \frac{19}{3} n_f$ . Here  $n_f$  is the number of flavors and  $Q$  is the hard physical momentum. High order corrections have higher powers of  $\beta_n$  with  $n \geq 3$ .

At large momentum  $Q$  gives

$$\alpha_s(Q) = \frac{4\pi}{\beta_0 \ln Q^2 / \Lambda^2} \left( 1 - \frac{2\beta_1}{\beta_0^2} \frac{\ln \ln(Q^2 / \Lambda^2)}{\ln(Q^2 / \Lambda^2)} + \dots \right) \quad (11)$$

This function is decreasing at large  $Q^2 \gg \Lambda^2$  as inverse power of  $\ln Q / \Lambda$ . The coefficient of this power is fixed by the two first orders of the expansion (10).

The parameter  $\Lambda$  is obtained from phenomenological calculation and is of order  $\Lambda_{\overline{\text{MS}}} = 200$  MeV for  $n_f = 5$ . This is valid in the  $\overline{\text{MS}}$  scheme one of the most used scheme in QCD. It is interesting that in the Monte Carlo HERWIG program the value of  $\Lambda$  is larger than the value at  $\overline{\text{MS}}$  scheme by a factor 1.57 for  $n_f = 5$ . It has been computed directly in the HERWIG Monte Carlo scheme by perturbative calculations valid at large  $x$ . This expression holds both for positive and negative  $Q^2$ . It is defined by (11) at two loops.

The form of  $\alpha_s(Q)$  is represented in the first part of Fig. 4. Comparison with data in various processes is given such as in  $e^+e^-$  collisions, in hadronic collisions, in heavy quark events. The maximal scale of  $Q$  considered is up to  $Q = 200$  GeV.

In the second part of Fig. 4 one has the average  $\alpha_s(M_Z)$  at the mass  $M_Z = 91.2$  GeV. Various measurements are here represented.

Here the  $\alpha_s(Q)$  determination is valid for  $Q$  larger than few GeV. The determination of  $\alpha_s(Q)$  is reduced at large  $Q$ . Here one expects that at large momentum in LHC the determination of  $\alpha_s(Q)$  will be rather good.

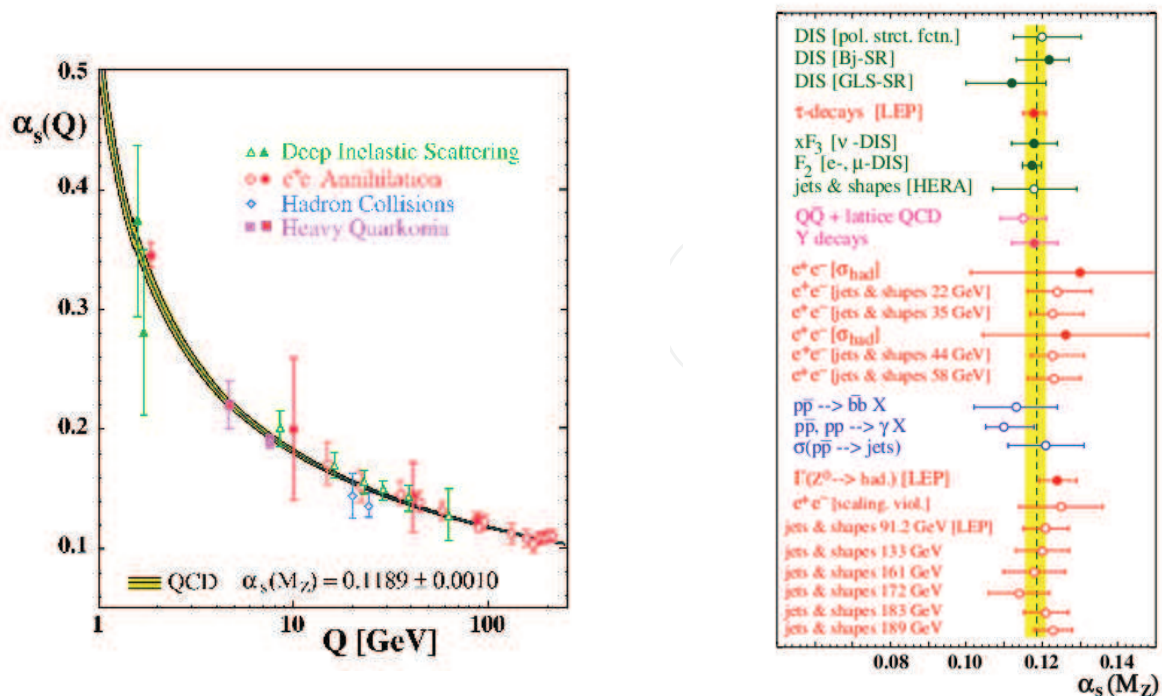


Fig. 4. Parton evolution in QCD. First part: the running coupling  $\alpha_s(Q)$  as function of  $Q$ . Second part: average  $\alpha_s(M_Z)$

#### 4.0.0.12 Parton evolutions in initial states.

Consider the initial state evolution with energy fraction  $x$  of final parton  $b$ . Here parton density  $D_{ba}(Q^2, x)$  evolves as in (5) and one needs to define the running coupling dependence on  $Q^2$ . QCD analysis at present scales defines  $Q$  as the transverse momentum of emitted initial state parton  $b$ . This is found from initial state emission at limited scale used by present machines, see (1).

At larger momenta one should use a more complex variable corresponding essentially to  $Q$  given by angle of emitted parton with respect to the incoming original one given by proton momentum. Experimental evidence of the relevance of this scale for  $Q$  is clear from various analysis, see (1).

There are complications when one reduces  $x$  to very small values, well below  $x \simeq 10^{-4}$ . Here the evolution is more complex than the one given in (14). The new equation in this region is more complex and involves more degree of freedom. The new formulation is described in (14) which is not considered in the HERWIG program.

#### 4.0.0.13 Parton evolutions in final states.

Consider now the final state evolution with energy fraction  $x$  of emitted parton  $b$ . Here parton density  $D_{ba}(Q^2, x)$  evolves as in (5). One needs to define the running coupling with respect to  $Q^2$ . QCD analysis at present scales defines  $Q$  as given by  $p_{bt}$  rescaled by incoming  $e_b$  and final energy  $E$ , i.e.  $Q = p_{bt} \times e_b/E \simeq e_b \theta_b$ . Here  $\theta_b$  is the angle of emitted parton  $b$ . This means that the new scale is essentially, for small momentum, of the order of the emitted parton transverse momentum. This rescaling is due to QCD calculations accounting for soft emitted gluon coherence, see (15).

This selection of the final state emission has been defined for many QCD quantities. The important point here is that the scale  $Q$  decreases as one decreases the emitted angle  $\theta_b$  and

the energy  $e_b$ . This last dependence is the crucial one. It is for instance responsible for the dependence on the multiplicity that we discuss now, see (1).

#### 4.0.0.14 Multiplicity.

In  $e^+e^-$  emission at energy  $E$  the parton multiplicity has been computed, see (15), and is given by

$$\langle N(Q) \rangle \simeq N_0 \left( \ln \frac{Q^2}{\Lambda^2} \right)^{\frac{\sqrt{N_c}}{2\pi\beta_0}} \exp \sqrt{\frac{2N_c}{\pi\beta_0} \ln \frac{Q^2}{\Lambda^2}} \quad (12)$$

with  $\Lambda$  the QCD scale. Here  $N_0$  is a normalization constant to be defined experimentally. It is the multiplicity evaluated at a scale  $Q_0$ . This involves again the QCD scale discussed before. In this expression we have neglected the two loop formulation. This is one of the most measured quantity in QCD, see Fig. 5.

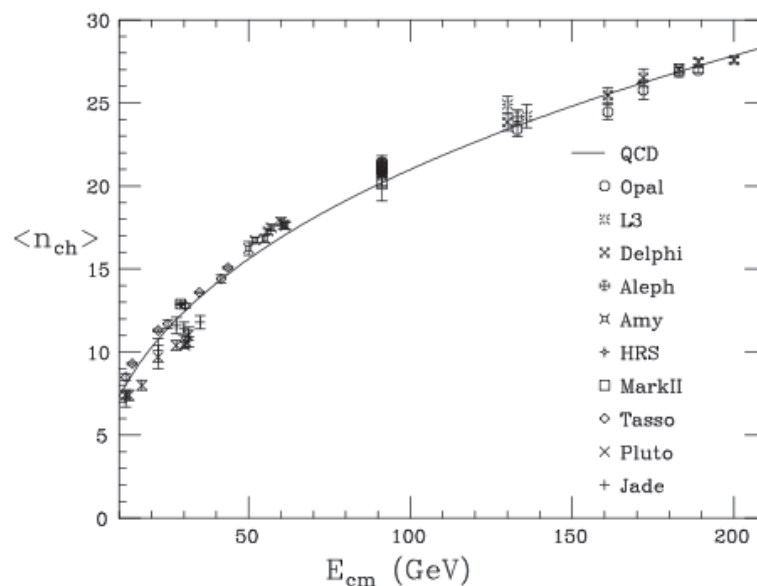


Fig. 5. Multiplicity

Total multiplicities will be measured at LHC for various channels. The agreement of data with (12) is expected to be very good.

#### 4.0.0.15 Preconfinement and hadron formation.

In the Monte Carlo evolutions many partons are produced in the final state. They have a color and they could generate hadrons made of color singlets. Then an important question is how these partons are organized in the final state and how color singlet partons are organized with small mass to form hadrons.

The reason that makes the mass of color singlet partons in QCD small, of order of  $M_0$ , is the presence of a Sudakov form factor which damps the mass. Indeed, the singlet emission of color partons (in the infinite  $N_c$  limit) contains this form factor which is fastly decreasing with total momentum. In this way one finds that color singlet partons could form a system of combined hadrons.

One checks by QCD evaluation, see (6), that in QCD color singlet partons are actually generated with small mass of order of  $M_0$ . In this case one could implement into HERWIG



calculation a reconstruction of hadrons. This reconstruction is reasonable but out of a formal treatment of QCD calculations.

To construct hadrons out of color singlet partons in HERWIG one uses this QCD property and looks into the Particle Data Book property, see (7), and identifies clusters of color singlet parton system.

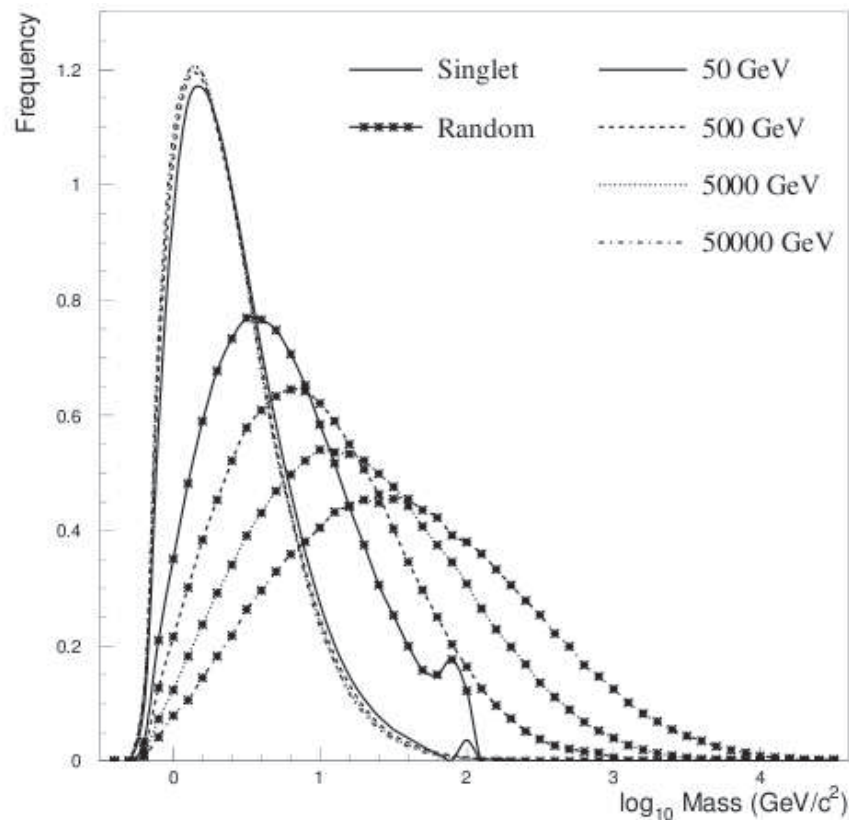


Fig. 6. Preconfinement

In Fig. 6 one sees the distribution in the mass of two partons in  $e^+e^-$  machine at various energies. The left line gives the distribution in the mass of color singlet. As one sees changing the total energy  $E$  the curves do not move and the distribution remains centered at  $M_0 = 2$  GeV.

The situation is different for the other lines which cluster two generic partons with no selection of color charge. They move as the total energy  $E$  increases and no hadron cluster could be formed.

#### 4.0.0.16 Non perturbative QCD assumptions.

After the described process of hadron formation in QCD, in HERWIG evolution one could explore other particle formations. They could involve Standard model processes as leptons, neutrinos and weak boson formations. One of the most important case is the Higgs boson generation with mass of order of hundred or hundred and fifty times the proton mass. They will confirm the simplest case of the Standard model. I recall that the Higgs meson is so important that is responsible for the formation of the mass of the weak bosons  $Z$  and  $W^\pm$ . Without the Higgs boson one has serious difficulties with the present version of the Standard model.

Other important processes which can be explored in HERWIG are non Standard model processes. They involves the supersymmetric models or generalization of the Standard model to implement new physics. See (16).

#### 4.0.0.17 Single proton distribution.

The data on  $W^+W^-$  production distribution is given at FermiLab up to total momentum  $p_t \simeq 70$  GeV, see Fig. 7. Here one plots the inclusive distribution  $\frac{d\sigma}{dp_t}$  in the transverse momentum of  $WW$  pair. See (2).

The curves are again compared with the analytical behavior. The agreement with experiments is quite well. One expects a similar behavior at LHC energy.

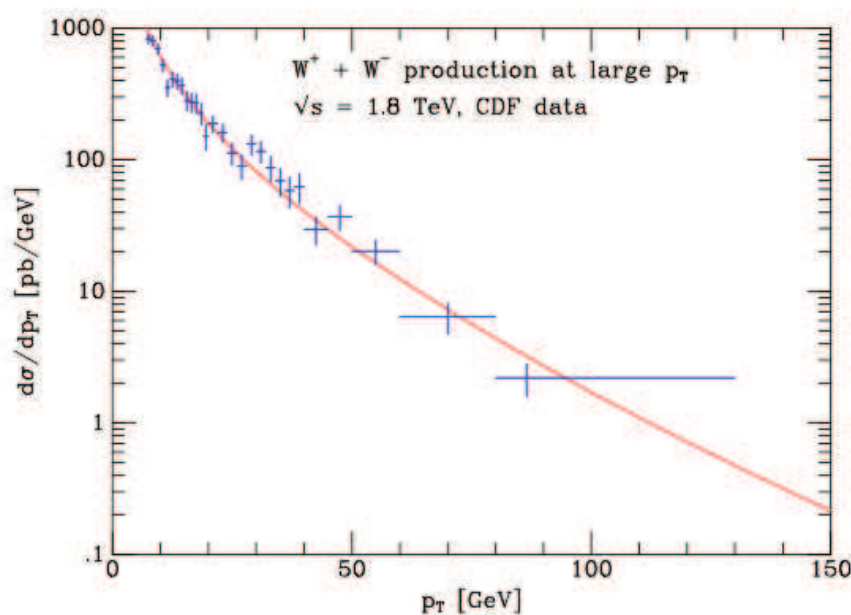


Fig. 7.  $WW$  inclusive distribution at FermiLab

#### 4.0.0.18 Particle clustering.

Consider the shape of the particle jet in Fig. 8. Measurements were done at  $e^+e^-$  machine at CERN. The jets are defined by giving a definite opening angle  $y_{\text{cut}}$ . This is defined by fixing momentum clustering as follows:

- given two emitted particles of momentum  $p_i$  and  $p_j$  one computes the variable  $y_{ij} = 2 \min\{E_i^2, E_j^2\}$  with  $E$  the energy of  $p$ ;
- if  $y_{IJ} = \min\{y_{ij}\} < y_{\text{cul}}$  with all previously analyzed momenta  $p_i$  and  $p_j$ , then particles  $I$  and  $J$  are put in a single particle  $k$  with  $p_k = p_I + p_J$  as a new momentum;
- replace until  $y_{ij} < y_{\text{cul}}$ . This defines the order of jets with previous resolution.

Jets are resolved according to parameters which define the number of jets given in first point above. Here one considers jet resolution given for 2, 3, 4, 5 jets. They are distributed according to Monte Carlo programs HERWIG and PYTIA. Data are taken from OPAL in  $e^+e^-$  collider at CERN, see (9).

The first distribution is done according to the resolution parameter  $y_{\text{cut}}$  given above. Mass is fixed at  $E = 91$  GeV at Opal at CERN, see Fig. 8. As one sees the average number of

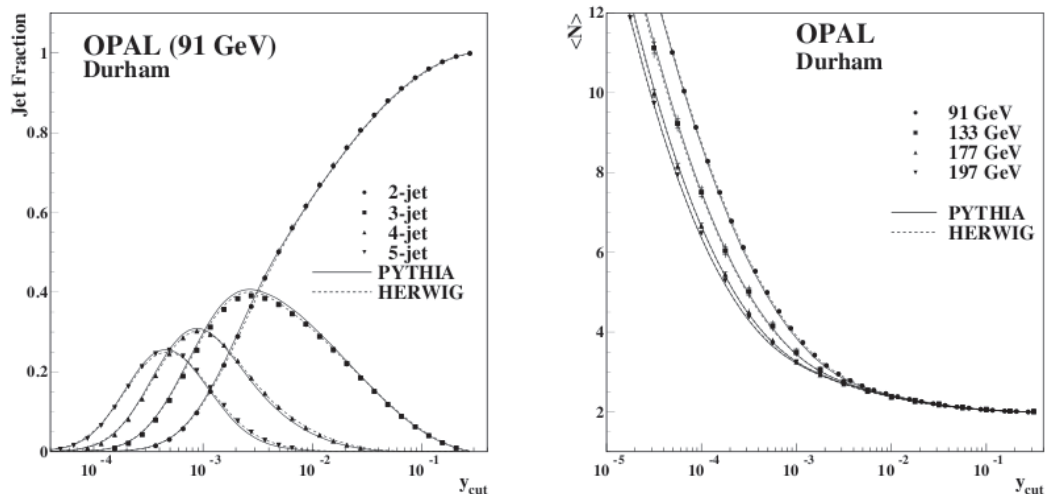


Fig. 8. Jet distribution at  $e + e^-$  accelerator.

jets increases as one decreases the resolution  $y_{\text{cut}}$ . That is the number of jets, as expected, increases as one decreases the resolution. The plots are computable in perturbation theory as for HERWIG. Of course, there is a minimum limit in the resolution  $y_{\text{cut}}$  to avoid particle identification.

The second plot represents the average values of jet resolution with respect to energy for the detector at 91, 133, 177, 197 GeV. The average number of jets decreases as one increases the total energy  $E$ .

#### 4.0.0.19 The Higgs boson.

The experimental observation of one or several Higgs bosons will be fundamental for a better understanding of the mechanism of electroweak symmetry-breaking. In the Standard model these are various expressions for the Higgs meson. This means to give a mass to  $Z$  and  $W^\pm$ . In particular there are indications from previous experiments at FermiLab and CERN for  $e^+e^-$  colliders that one has a Higgs meson mass between 100 and 150 GeV.

Here there are some important examples for the decay of standard Higgs meson. These data are taken from ATLAS studies, see (3);

- $H \rightarrow \gamma\gamma$  direct productions;
- $H \rightarrow \gamma\gamma$  from the associated production of  $W + H$ ,  $W + Z$  and  $t\bar{t} + H$ ;
- $H \rightarrow b\bar{b}$  from the observed production  $W + H$ ,  $Z + H$  and  $t\bar{t} + H$ ;
- $H \rightarrow ZZ \rightarrow$  and  $Z$  into two leptons;
- $H \rightarrow ZZ \rightarrow$  and  $ZZ$  into two leptons and two neutrinos;
- $H \rightarrow W^+W^-$  and  $H \rightarrow ZZ$  with Standard model decays.

In Fig. 9 we consider possible rates for Higgs production and decay. We report the determinations of the frequencies of the various channels by changing the  $H$  energy. The estimation is done by ATLAS group, see (1).

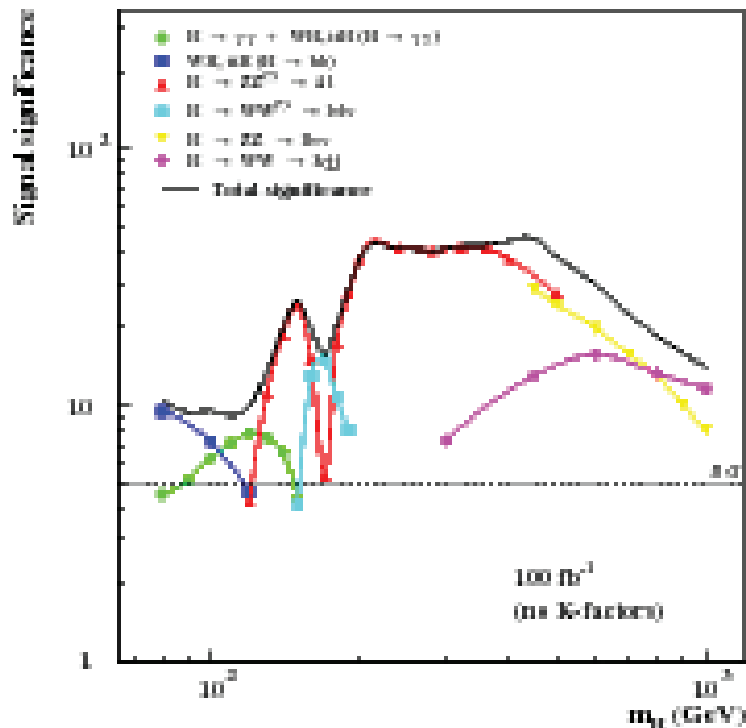


Fig. 9. Preview of particle measurements

#### 4.0.0.20 The Higgs boson in SUSY physics.

The supersymmetric standard model is a usual way to generalize the Standard model by including Supersymmetry, i.e. by adding a symmetry between bosons and fermions, see (16). The curves in the first part of Fig. 10 give  $1/\alpha(Q)$  for the normal Standard model. As one sees here in the case of the Standard model the three curves do not meet. They are close at an energy  $Q \sim 10^{15}$  GeV but do not meet. See details close to the expected mixing point.

In the case of SUSY model, see the second curve, data on  $1/\alpha(Q)$  are given for the three curves. At  $Q = 10^{15}$  GeV they actually meet and the model in principle can be unified. Actually the unification energy is rather high. There are various analysis of the SUSY model and there are various generalizations. See details near the mixing point.

The generalization of the Standard model and its analysis with HERWIG is used and analyzed in principle. Important generalizations involve theories beyond the Standard model. We do not enter here. See for example (17).

#### 4.0.0.21 Associated soft interactions.

In all hard collisions also soft interactions are involved and need to be considered for many measurements. These collisions are not considered here and could be found in the relevant references, see (4; 5).

## 5. Summary

The original formulation of the HERWIG program was stated in 1983, see (4). Later it was developed for various accelerators by using various QCD rules and their generalizations to the Standard model and beyond. At the moment it is used for the LHC accelerator. Large momenta are here involved to select very specific distributions. The search of Higgs is one

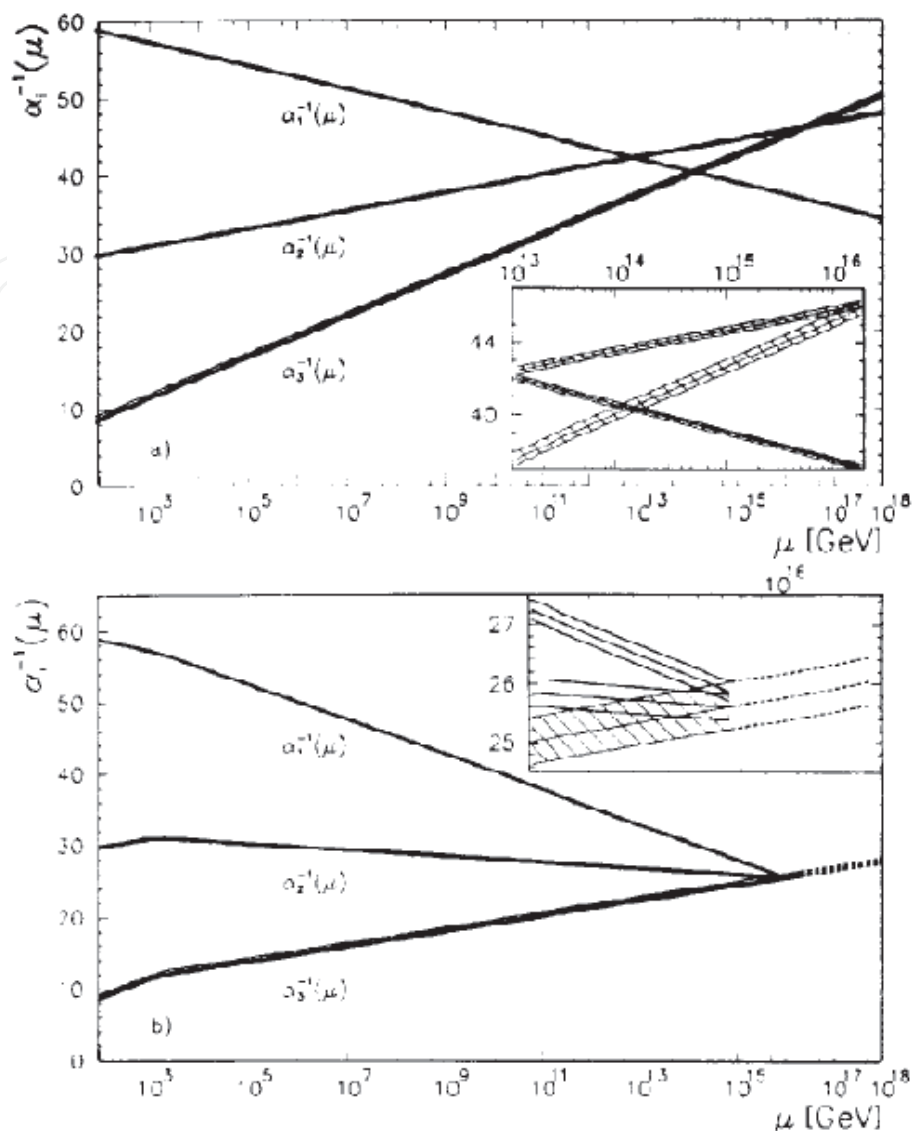


Fig. 10. SUSY unification for  $\alpha_s$

of the major point for the HERWIG program. It is important for setting the Standard model and the masses of  $Z$  and  $W^\pm$ . Very important at this LHC scale are the observations of other possible observables such as non QCD distributions in the Standard model and beyond.

All QCD perturbative calculations involved in the HERWIG program are obtained at leading level. Some important non leading corrections are here included in many computed quantities. Some important additions are discussed here.

The important point here is the presence of the hard scale  $Q_{\text{hard}}$ . These selected hard processes are under control of perturbative QCD analysis. Important processes are selected in this way. Higgs search is one of the crucial point which was intensively discussed here. Extensions to Standard model are easily treated here. Similarly for simple example beyond the Standard model.

An important point is the presence of the artificial parameter of the infrared cutoff  $M_0$ . It forces the absence of infrared divergences and is effectively close to the proton mass. This

parameter forces one to implement the presence of the physical hadrons. They are generated artificially by constructing hadron generation out of small mass color singlets of partons, see (4). The HERWIG program is actually based on this reconstruction of hadrons. Actually one can use different methods to generate hadrons but the essential basis are the same.

One element not considered in this study is the contributions from aspects that are beyond perturbative QCD such as the role of soft interaction within hard collisions. Their behavior is beyond perturbative QCD and then related to still not known quantities. They affect hard interactions and are clearly controlled.

Many pictures here shown are obtained from Bryan Webber transparencies. He was very important for my contribution to HERWIG.

## 6. References

- [1] Alfred H. Mueller, *Phys.Rev.D*4:150-155,1971;  
Yuri L. Dokshitzer, Dmitri Diakonov, S.I. Troian, *Phys.Rept.*58:269-395,1980;  
Guido Altarelli, *Phys.Rept.*81:1,1982;  
Antonio Bassetto, Marcello Ciafaloni, Giuseppe Marchesini, *Phys.Rept.*100:201-272,1983.
- [2] See for instance <http://www.fnat.gov>
- [3] See for instance <http://www.cern.ch>  
See also:  
<http://atlas.web.cern.ch/Atlas>  
<http://cms.web.cern.ch/cms>
- [4] G. Marchesini, B.R. Webber, *Nucl. Phys.* B238 (1984) 1;  
G. Marchesini, B.R. Webber, *Nucl. Phys.* B310 (1988) 461;  
G. Marchesini, B.R. Webber, G. Abbiendi, I.G. Knowles, M.H. Seymour and L. Stanco, *Phys. Commun.* 67 (1992) 465,  
G. Corcella, I.G. Knowles, G. Marchesini, S. Moretti, K. Odagiri, P. Richardson, M.H. Seymour and B.R. Webber, *JHEP* 0101 (2001) 010.
- [5] T. Sjostrand, S. Mrenna, P.Z. Skands, *JHEP* 0605:026,2006,  
A. Buckley, J. Butterworth, L. Lonnblad, H. Hoeth, J. Monk, H. Schulz, J. E. von Seggern, F. Siegert, L. Sonnenschein, arXiv:1003.0694.
- [6] D. Amati and G. Veneziano, *Phys.Lett.* B82 (1979) 87;  
A. Bassetto, M. Ciafaloni, G. Marchesini, *Phys. Lett.* B83 (1979) 207.
- [7] See the Particle Data Group at <http://pdg.web.cern.ch/pdg/> The Review includes a compilation and evaluation of measurements of the properties of the elementary particles. Evaluations of these properties are abstracted in summary tables.
- [8] HERA (Hadron-Electron Ring Accelerator) was an electron and positron accelerator at DESY. Its operation started in 1992 and finished in 2007. The two machines were H1 and Zeus. Electron energy was up to GeV and proton energy up to GeV.
- [9] The collider for  $e^+e^-$  was built at CERN. The total center of mass energy was used up to about 200 GeV. It operated from 1989 until 2000. Then it was replaced by LHC. There where four detectors: Aleph, Delphi, Opal and L3. See for instance the first part of (3).
- [10] S. Gieseke, D. Grellscheid, K. Hamilton, A. Ribon, P. Richardson, M.H. Seymour, P. Stephens, B.R. Webber, arXiv:hep-ph/0609306v1
- [11] V.N. Gribov, L.N. Lipatov. *Sov.J.Nucl.Phys.*15:438 (1972),  
G. Altarelli and G. Parisi. *Nucl.Phys.*B126:298 (1977),  
Yu. L. Dokshitzer. *JETP*, 46:641 (1977).
- [12] see for instance <http://www.cern.ch> and <http://www.lngs.infn.it/>

- [13] S. Catani, G. Marchesini, B.R. Webber, Nucl.Phys.B349:635-654,1991.
- [14] E.A. Kuraev, L.N. Lipatov, V.S. Fadin, Sov.Phys.JETP 45:199-204,1977;  
I.I. Balitsky, L.N. Lipatov, Sov.J.Nucl.Phys.28:822-829,1978;  
V.S. Fadin, L.N. Lipatov, Phys.Lett.B429:127-134,1998;  
M. Ciafaloni, D. Colferai, Phys.Lett.B452:372-378,1999.
- [15] A.H. Mueller, Phys. Lett. B104 (1981) 116;  
B.I. Ermolayev, V.S. Fadin, JETP Lett.33(1981) 269;  
A. Bassetto, M. Ciafaloni, G. Marchesini, A.H, Mueller, Nucl.Phys. B207 (1982) 189;  
Yu.L. Dokshitzer, V.S. Fadin, V.A. Khoze, Z.Phys.CI5 (1083) 325.
- [16] Examples of discussions of physics Beyond the Standard Model are discussed for instance in the first reference in (3).
- [17] See for instance U. Amaldi, W. de Boer, H. Furstenau, Phys.Lett.B260:447-455,1991.

IntechOpen



## **Applications of Monte Carlo Methods in Biology, Medicine and Other Fields of Science**

Edited by Prof. Charles J. Mode

ISBN 978-953-307-427-6

Hard cover, 424 pages

**Publisher** InTech

**Published online** 28, February, 2011

**Published in print edition** February, 2011

This volume is an eclectic mix of applications of Monte Carlo methods in many fields of research should not be surprising, because of the ubiquitous use of these methods in many fields of human endeavor. In an attempt to focus attention on a manageable set of applications, the main thrust of this book is to emphasize applications of Monte Carlo simulation methods in biology and medicine.

### **How to reference**

In order to correctly reference this scholarly work, feel free to copy and paste the following:

Giuseppe Marchesini (2011). HERWIG: a Monte Carlo Program for QCD at LHC, Applications of Monte Carlo Methods in Biology, Medicine and Other Fields of Science, Prof. Charles J. Mode (Ed.), ISBN: 978-953-307-427-6, InTech, Available from: <http://www.intechopen.com/books/applications-of-monte-carlo-methods-in-biology-medicine-and-other-fields-of-science/herwig-a-monte-carlo-program-for-qcd-at-lhc>

**INTECH**  
open science | open minds

### **InTech Europe**

University Campus STeP Ri  
Slavka Krautzeka 83/A  
51000 Rijeka, Croatia  
Phone: +385 (51) 770 447  
Fax: +385 (51) 686 166  
[www.intechopen.com](http://www.intechopen.com)

### **InTech China**

Unit 405, Office Block, Hotel Equatorial Shanghai  
No.65, Yan An Road (West), Shanghai, 200040, China  
中国上海市延安西路65号上海国际贵都大饭店办公楼405单元  
Phone: +86-21-62489820  
Fax: +86-21-62489821



© 2011 The Author(s). Licensee IntechOpen. This chapter is distributed under the terms of the [Creative Commons Attribution-NonCommercial-ShareAlike-3.0 License](#), which permits use, distribution and reproduction for non-commercial purposes, provided the original is properly cited and derivative works building on this content are distributed under the same license.

IntechOpen

IntechOpen